

## Precise Spectroscopy of the $3n$ and $3p$ Systems via the ${}^3\text{H}(t, {}^3\text{He})3n$ and ${}^3\text{He}({}^3\text{He}, t)3p$ Reactions at Intermediate Energies

K. Miki<sup>1,2</sup>, K. Kameya<sup>1,2</sup>, D. Sakai<sup>1,2</sup>, R. Urayama<sup>1,2</sup>, N. Imai<sup>3</sup>, S. Ishikawa<sup>4</sup>, S. Michimasa<sup>3</sup>, S. Ota<sup>3</sup>, M. Sasano<sup>2</sup>, H. Takeda<sup>2</sup>, T. Uesaka<sup>2</sup>, H. Haba<sup>2</sup>, M. Hara<sup>5</sup>, Y. Hatano<sup>5</sup>, T. Hayamizu<sup>2</sup>, N. Kobayashi<sup>6</sup>, A. Tamii<sup>6</sup>, S. Adachi<sup>7</sup>, T. Chillery<sup>3</sup>, M. Dozono<sup>2,8</sup>, Y. Fujikawa<sup>8</sup>, H. Fujita<sup>6</sup>, N. Fukuda<sup>2</sup>, T. Furuno<sup>6</sup>, J. Gao<sup>9</sup>, S. Goto<sup>10</sup>, S. Hanai<sup>3</sup>, S. Hayakawa<sup>3</sup>, Y. Hijikata<sup>2,8</sup>, K. Himi<sup>7</sup>, Y. Hirai<sup>10</sup>, J. W. Hwang<sup>11</sup>, M. Ichimura<sup>2,\*</sup>, D. Inomoto<sup>10</sup>, M. Inoue<sup>1,2</sup>, H. Kasahara<sup>10</sup>, T. Kawabata<sup>2,7</sup>, K. Kishimoto<sup>2,10</sup>, S. Kitayama<sup>1,2</sup>, K. Kusaka<sup>2</sup>, J. Li<sup>3</sup>, Y. Maeda<sup>12</sup>, Y. Maruta<sup>1,2</sup>, T. Matsui<sup>1,2</sup>, T. Matsuzaki<sup>2</sup>, S. Nakai<sup>1,2</sup>, H. Nishibata<sup>2,10</sup>, M. Otake<sup>2</sup>, Y. Saito<sup>1,2</sup>, H. Sakai<sup>2</sup>, A. Sakaue<sup>3</sup>, H. Sato<sup>2</sup>, K. Sekiguchi<sup>1,2</sup>, Y. Shimizu<sup>2</sup>, S. Shimoura<sup>3</sup>, L. Stuhl<sup>2,11</sup>, T. Sumikama<sup>2</sup>, H. Suzuki<sup>2</sup>, R. Tsuji<sup>2,8</sup>, S. Tsuji<sup>7</sup>, H. Umetsu<sup>1</sup>, Y. Utsuki<sup>1,2</sup>, T. Wakasa<sup>10</sup>, A. Watanabe<sup>1,2</sup>, K. Yako<sup>3</sup>, Y. Yanagisawa<sup>2</sup>, N. Yokota<sup>2,10</sup>, C. Yonemura<sup>2,10</sup>, K. Yoshida<sup>2</sup> and M. Yoshimoto<sup>2</sup>

(RIBF-SHARAQ11 Collaboration and RCNP-E502 Collaboration)

<sup>1</sup>*Department of Physics, Tohoku University, Sendai 980-8578, Japan*

<sup>2</sup>*RIKEN Nishina Center, Wako 351-0198, Japan*

<sup>3</sup>*Center for Nuclear Study, the University of Tokyo, Hongo, Tokyo 113-0033, Japan*

<sup>4</sup>*Science Research Center, Hosei University, Tokyo 102-8160, Japan*

<sup>5</sup>*Hydrogen Isotope Research Center, University of Toyama, Toyama 930-8555, Japan*

<sup>6</sup>*Research Center for Nuclear Physics, Osaka University, 10-1 Mihogaoka, Ibaraki, Osaka 567-0047, Japan*

<sup>7</sup>*Department of Physics, Osaka University, Toyonaka, Osaka 560-0043, Japan*

<sup>8</sup>*Department of Physics, Kyoto University, Kitashirakawa-Oiwake, Sakyo, Kyoto 606-8502, Japan*

<sup>9</sup>*School of Physics, Peking University, Beijing 100871, China*

<sup>10</sup>*Department of Physics, Kyushu University, Fukuoka 819-0395, Japan*

<sup>11</sup>*Center for Exotic Nuclear Studies, Institute for Basic Science, Daejeon 34126, Republic of Korea*

<sup>12</sup>*Faculty of Engineering, University of Miyazaki, Miyazaki 889-2192, Japan*

 (Received 10 January 2024; revised 23 April 2024; accepted 6 May 2024; published 3 July 2024)

To search for low-energy resonant structures in isospin  $T = 3/2$  three-body systems, we have performed the experiments  ${}^3\text{H}(t, {}^3\text{He})3n$  and  ${}^3\text{He}({}^3\text{He}, t)3p$  at intermediate energies. For the  $3n$  experiment, we have newly developed a thick Ti- ${}^3\text{H}$  target that has the largest tritium thickness among targets of this type ever made. The  $3n$  experiment for the first time covered the momentum-transfer region as low as 15 MeV/ $c$ , which provides ideal conditions for producing fragile systems. However, in the excitation-energy spectra we obtained, we did not observe any distinct peak structures. This is in sharp contrast to tetraneutron spectra. The distributions of the  $3n$  and  $3p$  spectra are found to be similar, except for the displacement in energy due to Coulomb repulsion. Comparisons with theoretical calculations suggest that three-body correlations exist in the  $3n$  and  $3p$  systems, although not enough to produce a resonant peak.

DOI: [10.1103/PhysRevLett.133.012501](https://doi.org/10.1103/PhysRevLett.133.012501)

**Background.**—Multineutron systems are being notably debated in the nuclear physics community [1]. The pivotal question is whether such neutral nuclear systems can form bound or resonant states. Recently, low-energy peak structures were discovered in the tetraneutron system [2,3], suggesting the possible existence of resonant states. However, interpretation of the origin of these peaks is hampered by the contradictory theoretical arguments. Understanding few-body multineutron systems is essential for understanding the interactions among neutrons and eventually the structures of neutron-rich nuclei and neutron stars. Herein, we focus on a  $3n$  system, the most fundamental

multineutron system with an odd neutron number, and present the first generation of the  $3n$  system under low-momentum-transfer conditions. To highlight the importance of our research on the  $3n$  system, we first review the current status of research on the  $2n$  and  $4n$  systems.

The search for multineutron systems is motivated by the fact neutrons can be strongly correlated with each other. Indeed, the interaction between low-energy two neutrons in  $S$  wave is attractive at distances of a few femtometers due to pion exchange, and it is free of Coulomb repulsion. As a result, a two-neutron system in vacuum forms a  ${}^1S_0$  virtual state [1] in close proximity to a bound state. In nuclei, the

existence of dineutron correlations has been revealed by recent studies in which two neutrons are spatially localized at the surfaces of neutron-rich nuclei [4,5]. There has been a particular focus on whether multineutron systems beyond just two neutrons may possess similar (quasi) stabilities and correlations.

These expectations have been greatly enhanced by two recent experiments of tetraneutron missing-mass spectroscopy performed at the RIKEN Radioactive-Isotope Beam Factory (RIBF). In the double-charge-exchange reaction  ${}^4\text{He}({}^8\text{He}, {}^8\text{Be})4n$  [2], four events in excess of the quasifree continuum background were found to be localized at an excitation energy of  $E_x = 0.83 \pm 1.41$  MeV, with a width of  $\Gamma < 2.6$  MeV (FWHM). Another peak structure with higher statistics was found at a consistent energy in the  $\alpha$ -knockout reaction  ${}^1\text{H}({}^8\text{He}, p{}^4\text{He})4n$  [3]; it was located at  $E_x = 2.37 \pm 0.58$  MeV and  $\Gamma = 1.75 \pm 0.37$  MeV. These consistent observations from different reaction mechanisms suggest the possible existence of a robust tetraneutron eigenstate. Additional experimental signatures were also reported in earlier research at GANIL [6] and in more recent work in Munich [7], where possible  $4n$  bound states were suggested.

However, these experimental results are puzzling in light of theoretical predictions. Our study is motivated by two conflicting groups of *ab initio* calculations. One is based on Faddeev-Yakubovsky or Gaussian-expansion formalisms (for example, see Refs. [8,9]), which do not produce a  $4n$  resonance pole. The other group is based on the methods such as quantum Monte Carlo or no-core shell model, which relies on some extrapolations in the continuum. These calculations suggest the existence of a  $4n$  resonance at energies close to the observed ones [10–12]. Apparently, the latter theory better describes the reality. However, the former group pointed out that such extrapolations inappropriately break analytic continuation on the complex-energy plane [1,13]. That group instead suggested different mechanism of peak formation for the  $\alpha$ -knockout reaction [14], although the peak in the double-charge-exchange spectrum still remained unexplained. Interestingly, the latter theory not only predicts the  $4n$  resonance but also predicts a  $3n$  resonance at even lower energies. For example, a no-core Gamow shell model calculation [12] predicts a  $4n$  resonance at 2.64 MeV, and a  $3n$  resonance at 1.29 MeV. Reliable experimental data for a  $3n$  resonance can therefore provide a crucial test of the validity of those theories.

The study of the  $3n$  system is thus of fundamental importance. The low-energy peaks have been observed for multineutrons with even neutron numbers ( $2n$  and  $4n$ ), but the  $3n$  system will be the first step in investigating those with odd neutron numbers. This will allow us to discuss whether two neutrons must have dineutron correlations to form peak structures. Additionally, since the  $3n$  system is a pure—and the simplest—*isospin*  $T = 3/2$  system, its energy spectrum may allow us to discuss the  $T = 3/2$  three-nucleon force (3NF).

Experimentally, there has not yet been sufficient investigation of  $3n$  systems. Previous studies, which were performed with the following reactions, reported no signature of a low-energy peak:  ${}^3\text{H}(n, p)3n$  at 14.4 MeV [15],  ${}^3\text{H}(t, {}^3\text{He})3n$  at 7.4 MeV/nucleon [16],  ${}^3\text{He}(\pi^-, \pi^+)3n$  [17,18], and  ${}^3\text{H}(\pi^-, \gamma)3n$  [19]. The biggest problem with the previous studies is that they all covered only the range of momentum transfer  $q_{c.m.} > \sim 100$  MeV/ $c$ . It is important to achieve low-momentum-transfer condition to produce fragile systems such as multineutrons, but such regions were not investigated in previous  $3n$  experiments.

In the present work, we have investigated the  $3n$  system via the reaction  ${}^3\text{H}(t, {}^3\text{He})3n$  at 170 MeV/nucleon. The minimum momentum transfer achieved in this reaction is as low as 15 MeV/ $c$  at a scattering angle of  $0^\circ$ , which corresponds to a  $3n$  center-of-mass kinetic energy of 40 keV. This energy scale is negligibly small compared with the possible  $3n$  resonance energy of a few MeV [12], and thus we can expect that produced  $3n$  systems are undisturbed by the reaction. We also emphasize that, at intermediate incident energies  $T > \sim 100$  MeV/nucleon, the charge-exchange reaction mechanism is well treated by the impulse approximation [20–22]. This means that initial- and final-state interactions between the projectile and the target system must be negligibly small, except for the charge-exchange process between the two nucleons. The  $3n$  system so produced is undisturbed also in this respect, which makes this reaction ideal for the search for  $3n$  resonance.

In addition to the reaction  ${}^3\text{H}(t, {}^3\text{He})3n$ , we have performed spectroscopy of the  $3p$  system using the reaction  ${}^3\text{He}({}^3\text{He}, t)3p$  at 140 MeV/nucleon. The  ${}^3\text{H}(t, {}^3\text{He})$  and  ${}^3\text{He}({}^3\text{He}, t)$  reactions are charge-symmetric with each other as shown in Fig. 1. This consistent study thus allows us to discuss the  $3n$  and  $3p$  systems on an equal footing. We are also able to discuss the extent to which charge symmetry holds and, owing to the chargeless conditions, the stability of the  $3n$  system.

*Experiments.*—The  ${}^3\text{H}(t, {}^3\text{He})3n$  experiment was performed at RIBF. The primary  ${}^4\text{He}$  beam was accelerated to 200 MeV/nucleon using the superconducting ring cyclotron and directed onto a 6-cm-thick  ${}^9\text{Be}$  production target. The secondary triton beam produced at 170 MeV/nucleon was purified using the BigRIPS fragment separator [23]

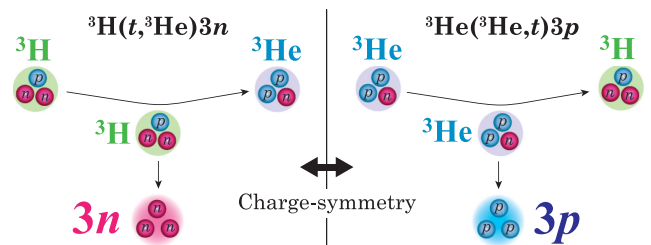


FIG. 1. Schematic illustrations of the  ${}^3\text{H}(t, {}^3\text{He})3n$  and  ${}^3\text{He}({}^3\text{He}, t)3p$  reactions, showing their charge symmetry.

and transported through the OEDO beamline [24,25] to secondary targets installed at the pivot point of the SHARAQ spectrometer [26]. The intensity of the triton beam was  $5 \times 10^7$  pps on the secondary target, and its purity was in excess of 99%. The  $^3\text{He}$  particles scattered from the target were momentum-analyzed using SHARAQ and were detected by the cathode-readout drift chambers and plastic scintillation counters installed at the focal plane. The resolutions of the excitation energy and scattering angle were 1.0 MeV (FWHM) and  $0.7^\circ$  (FWHM), respectively. The excitation energy is accurate to within 200 keV.

For the tritium target, we have newly developed a self-supporting thick Ti- $^3\text{H}$  target [27], and we have used it for the first time in this experiment. We stored an activity of 1.6 TBq of tritium in an 80- $\mu\text{m}$ -thick titanium foil, with the atomic loading ratio  $^3\text{H}/\text{Ti} = 1.5$ , which amounts to a tritium thickness of 3 mg/cm $^2$ . This is the thickest Ti- $^3\text{H}$  target ever made. During the subsequent analysis, this number was corrected for the decrease in the amount of the tritium due to the tritium  $\beta$  decay with a half-life of  $T_{1/2} = 12.32$  yr since the target was produced. Data were also accumulated using CH $_2$  and CD $_2$  targets for  $1n$  and  $2n$  missing-mass measurements, respectively, and using titanium, carbon, and blank-frame targets for background determinations.

The  $^3\text{He}(^3\text{He}, t)3p$  experiment was conducted at Research Center for Nuclear Physics (RCNP), Osaka University. The primary  $^3\text{He}$  beam was accelerated to 140 MeV/nucleon using the ring cyclotron and transported through the WS course beamline to the target position of the Grand Raiden spectrometer [28,29]. The tritons scattered from the target were momentum-analyzed using the spectrometer and were detected using the vertical drift chambers and plastic scintillation counters at the focal plane. The yields in another spectrometer—LAS, which was located at a scattering angle of  $55^\circ$ —were also recorded continuously and used for luminosity monitoring. The resolutions of excitation energy and scattering angle were 0.4 MeV (FWHM) and  $0.6^\circ$  (FWHM), respectively. The excitation energy is accurate to within 100 keV.

For the  $^3\text{He}$  target, we employed a cryogenic gas-target system. A target cell enclosed with 12- $\mu\text{m}$  Aramid windows (TORAY Mictron) was filled with  $^3\text{He}$  gas at a pressure of approximately 2 atm and cooled down to 9 K. A typical  $^3\text{He}$  thickness in the physics run was 5 mg/cm $^2$ . Data were accumulated also with CD $_2$ , C, Aramid, and empty-cell targets for gas-target thickness calibrations and background subtractions.

Figure 2 shows examples of the raw spectra. In the top panel, the red histogram is the  $(t, ^3\text{He})$  spectrum for the Ti- $^3\text{H}$  target, and the black histogram is that for the Ti target. A clear enhancement is observed in the continuum region for the Ti- $^3\text{H}$  target, which we attribute to the reaction on  $^3\text{H}$ . We note that the two peaks at  $E_x < 0$  MeV are identified by their kinematics and  $Q$  values as the

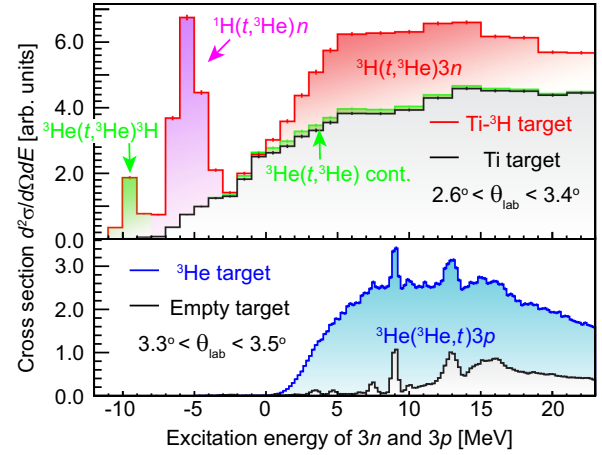


FIG. 2. Examples of the raw spectra for the  $^3\text{H}(t, ^3\text{He})3n$  reaction at  $3.0^\circ$  (top) and for the  $^3\text{He}(^3\text{He}, t)3p$  reaction at  $3.4^\circ$  (bottom). The errors in the experimental data are statistical only. See text for details.

$^1\text{H}(t, ^3\text{He})n$  and  $^3\text{He}(t, ^3\text{He})^3\text{H}$  reactions;  $^1\text{H}$  exists as an isotopic impurity of tritium, and  $^3\text{He}$  is produced by the beta decay of tritium. We subtracted the  $^1\text{H}$  component by using the same peak in the CH $_2$  spectra. The  $^3\text{He}(t, ^3\text{He})^3\text{H}$  peak is separated from the  $3n$  continuum due to the difference in  $Q$  values. The amount of  $^3\text{He}$  was less than 3% relative to  $^3\text{H}$ . Those peaks appear prominently because they are Gamow-Teller transitions and the cross sections are large. We determined the background from the  $^3\text{He}(t, ^3\text{He})$  continuum from the previous data [30] and subtracted it (green histogram). In the bottom panel, the blue histogram is the  $(^3\text{He}, t)$  spectrum for the  $^3\text{He}$  gas-target run, while the black histogram is for the empty target run. All the peaks in the former spectrum also exist in the latter and are attributed to the  $(^3\text{He}, t)$  reactions on  $^{12}\text{C}$ ,  $^{14}\text{N}$ ,  $^{16}\text{O}$ , and  $^{35,37}\text{Cl}$  in the Aramid foil.

**Results.**—The double-differential cross sections at the laboratory frame measured in the experiments are shown in Fig. 3 as functions of the excitation energies in the  $3n$  and  $3p$  systems at each momentum transfer  $q_{c.m.}$ . The zero of each excitation energy correspond to the total mass of three free nucleons. The red and blue histograms represent the missing-mass spectra for the  $^3\text{H}(t, ^3\text{He})3n$  and  $^3\text{He}(^3\text{He}, t)3p$  reactions, respectively. The error bars and shaded regions represent the statistical and systematic uncertainties, respectively. The data have additional systematic uncertainties in the overall normalizations, which are 9% for  $3n$  and 5% for  $3p$  spectra, respectively.

In sharp contrast to the tetra-neutron cases [2,3], we found no peak structure in either the  $3n$  or  $3p$  spectra in the region of measured excitation energies up to 20 MeV. This suggests that the three-nucleon system is nonresonant because at least one among the three nucleons miss the two-nucleon correlation. The cross sections increase from the threshold to approximately 10 MeV and then gradually decrease to

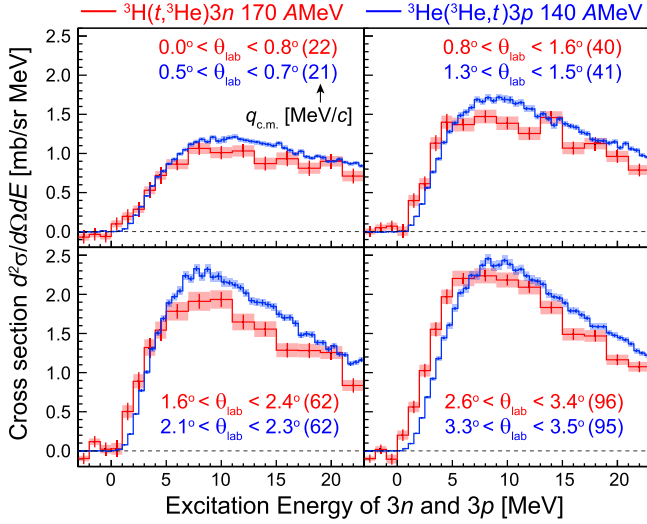


FIG. 3. Double-differential cross-section spectra for the  ${}^3\text{H}(t, {}^3\text{He})3n$  reaction at 170 MeV/nucleon (red) and for the  ${}^3\text{He}({}^3\text{He}, t)3p$  reaction at 140 MeV/nucleon (blue). The error bars and shaded regions represent the statistical and systematic uncertainties, respectively (additional normalization uncertainties are explained in the text). The numbers in parentheses represent the average momentum transfers  $q_{c.m.}$  [MeV/c].

higher excitation energies. As Coulomb repulsion is absent, it was expected that the cross section for  $3n$  would be more enhanced at low energies relative to that of  $3p$ . However, our actual data reveal that the difference appears as a shift of  $3n$  spectra toward the lower-energy side. Except for this energy shift, the overall shapes of the two distributions are similar. This is also different from the  $2n$  and  $2p$  cases, where a virtual-state peak structure is much more enhanced in the  $2n$  [31] than in the  $2p$  system [32].

*Discussion.*—To interpret the experimental cross-section distributions, we introduce two types of theoretical calculations. One is based on a quasifree formalism that reflects the phase-space distributions of the  $3n$  or  $3p$  systems in the final states [33]. This formalism is simple, but it is useful for figuring out the qualitative features of the observed  $3n$  and  $3p$  systems. We investigated the two extreme cases of “no correlation” and “2-body correlation.” In the no-correlation calculation, each nucleon scatters freely into plane-wave functions. In the case of two-body correlation, two of the nucleons form a quasibound state, and the system scatters into a  $2 + 1$  configuration. The other wave functions—for  ${}^3\text{He}$  and the tritons—are described by Gaussian form factors with radius parameters that are consistent with the measured charge distributions. We treated the reaction mechanism using the plane-wave impulse approximation (PWIA), with the effective nucleon-nucleon interaction taken from Ref. [34].

The top panels in Fig. 4 compare the results of these calculations with the experimental  ${}^3\text{H}(t, {}^3\text{He})3n$  spectra. The left and right panels are for the laboratory scattering

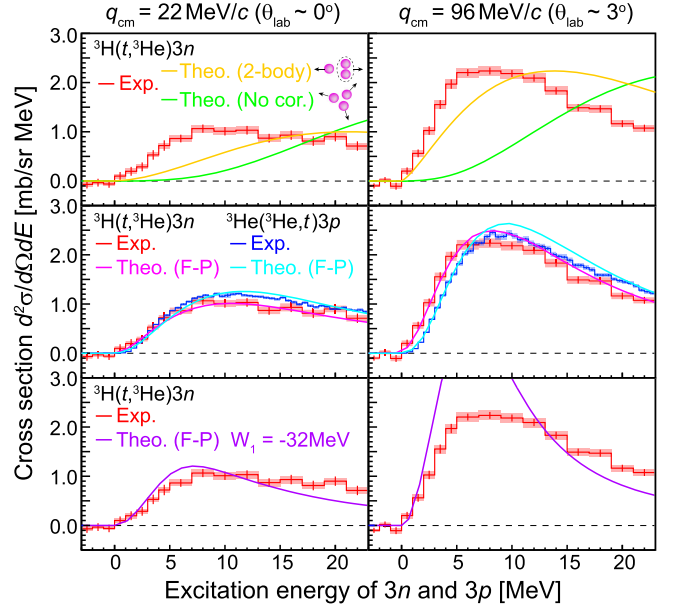


FIG. 4. Comparison of the theoretical calculations with the experimental  ${}^3\text{H}(t, {}^3\text{He})3n$  and  ${}^3\text{He}({}^3\text{He}, t)3p$  spectra at two momentum transfers (left and right). The experimental data are taken from Fig. 3. The theoretical calculations are the quasifree calculations (top), and the F-P calculations without (middle) and with (bottom) a phenomenological 3NF. See text for details.

angles  $\theta_{\text{lab}} \sim 0^\circ$  and  $\theta_{\text{lab}} \sim 3^\circ$ , respectively. The theoretical calculations are normalized so that their maximum cross sections agree with the experimental data at  $\theta_{\text{lab}} \sim 3^\circ$ . The peak energies of the no-correlation calculation (green) are located around 30 MeV, which is far beyond the experimental results (red). In the calculation of two-body correlation (yellow), the peak energies are located at a lower excitation energy around 15 MeV than those of green lines. However, the experimental distributions are located at even lower energies than those obtained from these two-body correlation calculations, which implies the existence of three-body correlations in the  $3n$  system.

For further quantitative discussion, we introduce more detailed calculations based on an *ab initio* method. In this formalism [35,36], the response functions for the transition from the three-nucleon bound state  ${}^3\text{H}$  ( ${}^3\text{He}$ ) to the  $3n$  ( $3p$ ) continuum states are calculated using the Faddeev formalism with the realistic interaction Argonne  $v_{18}$  [37], and the full correlations in the  $3n$  or  $3p$  system are properly considered. Effects of the Coulomb interactions are also taken into account adequately in this formalism, as shown in the previous studies on proton-deuteron scattering [38] and the  ${}^3\text{He}(p, n)3p$  reaction [35]. The present calculation includes the contributions of the  $3n$  and  $3p$  wave functions with the spin parities of  $J^\pi = 1/2^\pm, 3/2^\pm$ , and  $5/2^\pm$ , which dominate the cross section over the measured angular range. It has been shown in a previous study [36] that the  $3n$  system does not have a resonance pole close

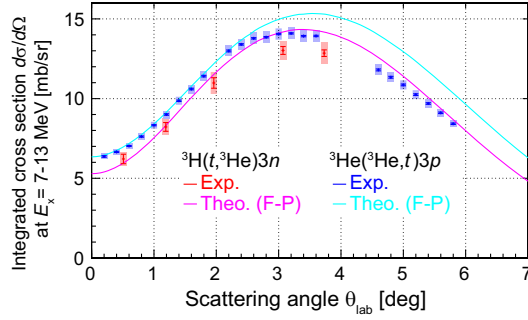


FIG. 5. Angular distributions of cross sections integrated over  $E_x = 7\text{--}13$  MeV. The errors in the experimental data are described in the caption of Fig. 3. See text for details.

to the physical region in this model. For the reaction mechanism, we again employed the PWIA, and constructed the effective nucleon-nucleon interaction in the reaction from the results of a phase-shift analysis of nucleon-nucleon scattering (PWA93) [39]. Hereafter, we refer to this model as the Faddeev-PWIA (F-P) calculation. The calculations are not normalized when comparing them with the experimental data.

The results are presented in the middle panels of Fig. 4. The F-P calculations for  ${}^3\text{H}(t, {}^3\text{He})3n$  (pink) and  ${}^3\text{He}({}^3\text{He}, t)3p$  (cyan) show  $E_x$  distributions similar to the experimental ones (red and blue, respectively). By treating the full correlations among three-nucleon systems, these calculations can reproduce the experimental peak energy remarkably well without a resonance pole near the physical region.

More quantitatively, we observe some differences between the calculation and experimental data. This is clearly depicted in Fig. 5, which shows the angular distribution of the cross sections integrated over the peak region  $E_x = 7\text{--}13$  MeV. Relative to the experimental data, the  ${}^3\text{He}({}^3\text{He}, t)3p$  calculation overestimates the cross section and peaks at larger angle. To provide a fully quantitative description of the considered reactions, the present formalism must be further refined. The  ${}^3\text{H}(t, {}^3\text{He})3n$  calculation exhibits a similar trend, although the significance of the difference is lower due to the larger systematic error in the experimental data.

Finally, we tested a 3NF contribution by employing a simple model. In Ref. [8], the authors tried to produce the  $4n$  resonance by introducing a strong phenomenological 3NF. This 3NF has a free parameter  $W_1$  that represents the strength of the long range part. By setting  $W_1$  to a very large value of  $-32$  MeV, they obtained a resonance pole in a  $4n$  system at the energy of the experimental observations around  $E_x = 1\text{--}2$  MeV. To test such possibility of strong 3NF effects in the  $3n$  case, we show the  $3n$  calculations using the same 3NF parameter (purple) in the bottom panels of Fig. 4. This 3NF introduces an enhanced peak structure at the larger angle, which degrades the consistency with the experimental data (red). This 3NF parameter

is obviously inappropriate. Indeed, it has previously been reported that such a strong 3NF destroys the low-lying structures of  ${}^4\text{H}$ ,  ${}^4\text{He}$ , and  ${}^4\text{Li}$  [8]. Not only in those static systems, the present study also rejects such a strong 3NF effect in the  $3n$  system including in its production dynamics.

*Summary and perspectives.*—To search for peak structures in the  $3n$  and  $3p$  energy spectra, we performed the experiments  ${}^3\text{H}(t, {}^3\text{He})3n$  at 170 MeV/nucleon and  ${}^3\text{He}({}^3\text{He}, t)3p$  at 140 MeV/nucleon, respectively. Our  ${}^3\text{H}(t, {}^3\text{He})3n$  spectra provide the first data for  $3n$  systems produced at momentum transfers lower than  $\sim 100$  MeV/ $c$  and down to 15 MeV/ $c$ . In the measured spectra, we did not find any peak structure in either the  $3n$  or  $3p$  systems. The F-P calculations—which do not have  $3n$  resonance poles in the observable regions—reproduced the overall  $E_x$  distributions of the experimental cross sections.

We have observed differences between the F-P calculations and the experimental data. It is important to improve the theoretical formalism because there is still some chance of constraining the  $T = 3/2$  3NF from these differences. Ideally, one should perform a full six-body reaction calculation that includes both the projectile and the target system for the  ${}^3\text{H}(t, {}^3\text{He})3n$  and  ${}^3\text{He}({}^3\text{He}, t)3p$  reactions. If that is beyond the reach of current theoretical techniques, one could still consider improving the current formalism by considering distortion effects as well as knock-on exchange contributions [40] in the impulse approximation framework. One could also try more realistic expressions for the 3NF—such as one based on an effective chiral Lagrangian—to investigate the sensitivity of the spectra to the 3NF more quantitatively. From an experimental perspective, it is beneficial to reduce systematic errors in particular for  $3n$  data. Improving the system that monitors the amount of the highly intense triton beam, which currently dominates the contribution to the systematic error, is worth considering.

The authors appreciate the staff of RIKEN Nishina Center and CNS, University of Tokyo for the operation of RIBF. They also thank the radiation safety group at RIBF and the staff of the University of Toyama for the cooperation in the handling of the highly radioactive tritium target. The authors are grateful to the staff of RCNP for their efforts to provide a clean and stable beam. Part of numerical calculations in this work was performed using computational resources of the Laboratory provided by the Research Center for Computing and Multimedia Studies, Hosei University (Project ID: LAB-464). This work was supported by a joint research program of the Hydrogen Isotope Research Center, Organization for Promotion of Research, University of Toyama (HRC2019-04 and HRC2020-08), by Korean grants from Institute for Basic Science (IBS-R031-D1 and IBS-R031-Y2), and by JSPS KAKENHI Grants No. JP17H04833 and No. JP20H01924.

\*Deceased.

- [1] F. M. Marqués and J. Carbonell, *Eur. Phys. J. A* **57**, 105 (2021).
- [2] K. Kisamori, S. Shimoura, H. Miya *et al.*, *Phys. Rev. Lett.* **116**, 052501 (2016).
- [3] M. Duer, T. Aumann, R. Gernhäuser *et al.*, *Nature (London)* **606**, 678 (2022).
- [4] A. B. Migdal, *Sov. J. Nucl. Phys.* **16**, 238 (1973).
- [5] Y. Kubota, A. Corsi, G. Authelet *et al.*, *Phys. Rev. Lett.* **125**, 252501 (2020).
- [6] F. M. Marqués, M. Labiche, N. A. Orr *et al.*, *Phys. Rev. C* **65**, 044006 (2002).
- [7] T. Faestermann, A. Bergmaier, R. Gernhäuser *et al.*, *Phys. Lett. B* **824**, 136799 (2022).
- [8] E. Hiyama, R. Lazauskas, J. Carbonell, and M. Kamimura, *Phys. Rev. C* **93**, 044004 (2016).
- [9] A. Deltuva, *Phys. Lett. B* **782**, 238 (2018).
- [10] A. M. Shirokov, G. Papadimitriou, A. I. Mazur, I. A. Mazur, R. Roth, and J. P. Vary, *Phys. Rev. Lett.* **117**, 182502 (2016).
- [11] S. Gandolfi, H.-W. Hammer, P. Klos, J. E. Lynn, and A. Schwenk, *Phys. Rev. Lett.* **118**, 232501 (2017).
- [12] J. G. Li, N. Michel, B. S. Hu, W. Zuo, and F. R. Xu, *Phys. Rev. C* **100**, 054313 (2019).
- [13] A. Deltuva and R. Lazauskas, *Phys. Rev. Lett.* **123**, 069201 (2019).
- [14] R. Lazauskas, E. Hiyama, and J. Carbonell, *Phys. Rev. Lett.* **130**, 102501 (2023).
- [15] V. Ajdačić, M. Cerineo, B. Lalović *et al.*, *Phys. Rev. Lett.* **14**, 444 (1965).
- [16] G. G. Ohlsen, R. H. Stokes, and P. G. Young, *Phys. Rev.* **176**, 1163 (1968).
- [17] J. Sperinde, D. Fredrickson, R. Hinkins, V. Perez-Mendez, and B. Smith, *Phys. Lett.* **32B**, 185 (1970).
- [18] M. Yuly, W. Fong, E. R. Kinney *et al.*, *Phys. Rev. C* **55**, 1848 (1997).
- [19] J. Miller, J. Bistirlich, K. Crowe *et al.*, *Nucl. Phys.* **A343**, 347 (1980).
- [20] G. Perdikakis, R. G. T. Zegers, S. M. Austin *et al.*, *Phys. Rev. C* **83**, 054614 (2011).
- [21] M. Ichimura, H. Sakai, and T. Wakasa, *Prog. Part. Nucl. Phys.* **56**, 446 (2006).
- [22] K. Miki, H. Sakai, T. Uesaka *et al.*, *Phys. Rev. Lett.* **108**, 262503 (2012).
- [23] T. Kubo, K. Kusaka, K. Yoshida *et al.*, *IEEE Trans. Appl. Supercond.* **17**, 1069 (2007).
- [24] S. Michimasa, T. Chillery, J. Hwang *et al.*, *Nucl. Instrum. Methods Phys. Res., Sect. A* **540**, 194 (2023).
- [25] S. Michimasa, J. Hwang, K. Yamada *et al.*, *Prog. Theor. Exp. Phys.* **2019**, 043D01 (2019).
- [26] T. Uesaka, S. Shimoura, H. Sakai *et al.*, *Prog. Theor. Exp. Phys.* **2012**, 03C007 (2012).
- [27] K. Miki, Y. Utsuki, M. Hara, Y. Hatano, N. Imai *et al.*, *Nucl. Instrum. Methods Phys. Res., Sect. A* **1056**, 168583 (2023).
- [28] T. Wakasa, K. Hatanaka, Y. Fujita *et al.*, *Nucl. Instrum. Methods Phys. Res., Sect. A* **482**, 79 (2002).
- [29] M. Fujiwara, H. Akimune, I. Daito *et al.*, *Nucl. Instrum. Methods Phys. Res., Sect. A* **422**, 484 (1999).
- [30] A. Celler, S. Yen, W. P. Alford *et al.*, *Phys. Rev. C* **47**, 1563 (1993).
- [31] C. Bäumer, D. Frekers, E.-W. Grewe *et al.*, *Phys. Rev. C* **71**, 044003 (2005).
- [32] B. J. Morton, E. E. Gross, E. V. Hungerford *et al.*, *Phys. Rev.* **169**, 825 (1968).
- [33] M. Ichimura, Computer code PROD3N (2016).
- [34] M. A. Franey and W. G. Love, *Phys. Rev. C* **31**, 488 (1985).
- [35] S. Ishikawa, *Prog. Theor. Exp. Phys.* **2018**, 013D03 (2018).
- [36] S. Ishikawa, *Phys. Rev. C* **102**, 034002 (2020).
- [37] R. B. Wiringa, V. G. J. Stoks, and R. Schiavilla, *Phys. Rev. C* **51**, 38 (1995).
- [38] S. Ishikawa, *Phys. Rev. C* **80**, 054002 (2009).
- [39] V. G. J. Stoks, R. A. M. Klomp, M. C. M. Rentmeester, and J. J. de Swart, *Phys. Rev. C* **48**, 792 (1993).
- [40] W. G. Love and M. A. Franey, *Phys. Rev. C* **24**, 1073 (1981).